ScienSage

Journal of Advanced Scientific Research

Available online through http://www.sciensage.info

ISSN
0976-9595
Research Article

INFLUENCE OF Ba SUBSTITUTION IN $SrTiO_3$ PEROVSKITE: STUDIES OF PHOTOCATALYSIS AND CATALYTIC BIGINELLI REACTION

Teotone Vaz*[1], Ashwini S. More[2], Janesline Fernandes[1], S. M. Gurav[3]

[1]*Dept. of Chemistry, St. Xavier's College, Mapusa Goa, India*

[2]*P.G. Dept. of Chemistry, St. Xavier's College, Mapusa, Goa, India*

[3]*Dept. of Chemistry, Govt. College of Arts, Sc., and Com, Quepem, Goa, India*

**Corresponding author: teovaz18@gmail.com*

ABSTRACT

Crystalline Barium substituted $Sr_{1-x}Ba_xTiO_3$ (x =0.0, 0.04, and 0.08) system nanomaterials were successfully prepared via modified sol-gel citrate precursor technique at 800°C temperatures. A comparative study of the structural, morphological, optical properties and catalytic activity is reported. Synthesized nanomaterials were analyzed by X-ray diffraction and FTIR. Pristine $SrTiO_3$ compound found to be cubic structure. On substitution of Ba in Sr-site, the slight distortion in XRD diffraction peaks were observed. Photo-catalytic efficiency using UV-Visible Spectroscopy was investigated by photo-degradation of synthetic dye in Laundry wastewater employing solar light, and found to be promising photo-catalysts. The catalytic potentiality was also explored for the synthesis of dihydropyrimidinone using Biginelli reaction and the product was found to increase upto 20% for $Sr_{0.2}Ba_{0.8}TiO_3$ with the highest concentration of Barium.

Keywords: Strontium Barium titanate, Sol-gel, XRD, Biginelli reaction, Photo-catalysis.

1. INTRODUCTION

The perovskite-type titanates, $ATiO_3$ (A = Sr and or Ba ion) exhibit an array of applications in sensors, actuators, microelectronics, solar cells, H_2 production, resistive O_2 gas sensors, and a promising candidate as a photocatalyst. In general, many perovskites possess cubic or nearly cubic in structure but can incorporate ions of various size and charge, showing great flexibility of structures with the substitution in A and/or B- site, leading to fascinating large scale applications. The substitution of ions, leading to deviation from ideal stoichiometry resulted in altering the electronic properties. By suitable changes in composition by doping or substitution, one can modify the most significant electroceramic dielectric $BaTiO_3$ phase in the industry, into metallic conductors, superconductors. The Lanthanide or alkaline earth metal ions at A-site support the framework stabilizes the system, and hence the size of these ions defines the octahedral structural transformations, which in turn decides the physical properties, governs the electronic state, and the phase transition [1-6].

Recently the scientists have dedicated more interest towards exploring a new type of semiconducting materials for use in the photodegradation of polluting matter. Semi-conducting materials with a bandgap of between 1.4 and 3.8 eV are potential photocatalytic materials and useful to reduce pollutants because they illustrate the simple condition to utilize natural or artificial irradiation [7]. The photo-degradation of the organic pollutants can be achieved by direct oxidation via oxidative species produced on the surface of photo-catalyst material on excitation. The performance efficiency of photo-catalyst can be enhanced by photo-generated charge carriers in the material and also by several other modifications such as crystallographic phase, active sites on the surface of the material, mixing with semiconducting materials, and by doping. The perovskite crystal structure provides a good framework, facilitating the tuning of bandgap values to enable solar light absorption and band edge potential suitable for specific photocatalytic reactions. Furthermore, the distorted lattice perovskite compounds strongly influence the separation of photogenerated electron-hole carriers. The Titanate class of materials has shown excellent visible-light photocatalytic activity [8-12].

The structure, particle size, and potential applications are strongly influenced by synthetic strategy. Most of

the photocatalyst perovskite materials are still produced with solid-state technique, but it is not easy to synthesize these materials in their pure bulk form, due to the unexpected presence of minor intermediate crystalline impurity phases. It is possible to prepare them comparatively in the pure form either by modified conventional ceramic, co-precipitation, hydrothermal, auto-combustion and also by other modern techniques like sonochemical, microwave-assisted, electro-spinning techniques. [3, 9-12]. Although, most of the methods employed have their limitations, the sol-gel precursor technique, which involves the complexing of cations in an aqueous-organic medium, making use of low-cost precursors resulting in the distribution of homogenous ions at the molecular level. Modification of sol-gel method, by using Citric acid as a complexing agent, serve the purpose of keeping metals in dissolved form and also maintaining acid pH [13-17]. Though the structural properties of pristine $SrTiO_3$, and substituting Sr ions with other alkaline earth metal like Ba ions have been reported [15-17], but to our knowledge, there are scanty literature reports available for such systems, study their effects on the structure and their impact on the catalytic properties of the material in organic synthesis. The objective of this work is to synthesize pristine $SrTiO_3$ and Ba-substituted $Sr_{1-x}Ba_xTiO_3$ (x = 0.0, 0.04, and 0.08) system nano-materials, via a simple, and reliable sol-gel citrate precursor approach to fabricate controllable crystal structure and to investigate the influence of Ba ion on their photocatalytic activity and Biginelli reaction.

2. MATERIAL AND METHODS

2.1. Sol-gel citrate precursor synthesis

Stoichiometrically calculated amounts of hydrated salts of Strontium nitrate and/or Barium nitrate were dissolved in pure water. The required amount of Titanium tetrachloride was dissolved separately in 10% HCl and added slowly with constant stirring to the above solution at 60°C . Citric acid was dissolved in pure water, was added slowly to obtain respective metal citrate precursor precipitate maintaining the pH neutral by adding 1:1 Ammonium hydroxide solution. All the above AR grade raw materials were used as procured. The temperatures were raised for the slow evaporation and reduced the quantity to half, leading to the setting of the desirable gel. The content was kept overnight and slowly decomposed by raising the temperature up to 200°C. A fluffy mass was then subjected to heat treatment at 400°C in the air till free from all carbonaceous matter. The solid powders were ground, calcined in stages at 600 and 800°C for a total duration of 8-10 h, and were furnace cooled, powdered, and stored in airtight containers for characterization.

2.2. Material characterization

X-ray Powder Diffraction (XRD) technique was used for structural and crystallographic analysis of as-synthesized materials. The diffraction analysis was carried out on Rigaku Ultima IV X-ray diffractometer (tabletop, Japan) using Cu-Kα line (1.5418 Å) filtered through Ni absorber at room temperature (R.T.). The 2θ range used was 20-80°. All the diffraction peaks in the observed XRD pattern can be clearly indexed by the respective I.C.D.D. file. Fourier Transformed Infrared (FTIR) spectra were recorded on a Shimadzu FTIR spectro-photometer (Model 8101A) in the range of 500-1500 nm with an approximate 1% sample embedded in KBr pellet.

$SrTiO_3$ compounds are well-known photo-catalysts. The catalytic activity of the materials under investigation was explored for the two model reactions. 1) One-pot synthesis of dihydropyrimidinone derivatives and 2) the photo-catalytic capacity of the nano-catalyst materials under investigation was tested on the laundry waste (LW) water containing synthetic dyes as a model reaction for photo- degradation of organic pollutants.

2.2.1. The Biginelli reaction as a model catalytic application

A solution of Benzaldehyde (10 mmol, 1.06 g), ethylaceto acetate (13mmol, 1.69 g), and urea (15 mmol, 0.90g) were refluxed at 85- 90°C in ethanol in the presence of materials (0.2 g) under investigation, for 3 h. On completion of the reaction, the catalyst was filtered off from the mixture, and the filtrate was collected in crushed ice. The crude product obtained was re-crystallized using ethyl acetate. The synthesized product was identified by comparison of melting point (mp) and the spectral data (FTIR) with the literature. The reaction follows the below scheme.

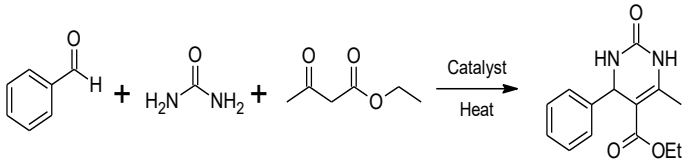

Dihydropyrimidinone

2.2.2. *Photo-catalytic degradation of synthetic dye in the laundry wastewater*

The degradation was carried out with 100mL of laundry wastewater (LWW) containing 0.1 g of the nanocatalyst material. The progress of dye degradation in LWW was monitored by measuring the absorbance at their characteristic λ_{max} of 440 nm. The experiments were performed using solar radiation at around noon and repeated on the next day for the consistency of results. Aliquots of the solutions were taken at the end of every 30 min time of the irradiation and analyzed with the UV - visible spectroscopy. The percentage of LWW degradation was studied by plotting absorbance versus time (min).

3. RESULTS AND DISCUSSION

3.1. Phase formation check by XRD

X-ray diffraction is a technique often used to study crystallinity, crystal structure, and atomic spacing. The prepared compositions were characterized by X-ray powder diffractograms. The d_{hkl} and 2θ values obtained were compared with the values reported in the literature and found to be in good agreement. Since the d_{hkl} value of the intermediate x = 0.4, and 0.8 compositions are not reported in the literature, the values were compared with the end compositions $SrTiO_3$ and $BaTiO_3$. Fig. 1 shows the XRD plots for the investigated materials. Our results of X-ray analysis showed that $SrTiO_3$ and $Sr_{0.6}Ba_{0.4}TiO_3$ could be clearly indexed to cubic perovskite structure (JCPDS data file no. 34-0411). The diffraction pattern of $Sr_{0.2}Ba_{0.8}TiO_3$ compound is indexed to the slightly distorted cubic perovskite structure and compared with $BaTiO_3$, in accordance with other published work [17, 18]. The diffraction peaks were readily indexed and the absence of additional peaks of oxides of Sr, Ba or Ti, suggesting that the purity of prepared materials. The sharp diffraction peaks and the high value of intensity ratio between the two highest peaks confirm better crystallinity of the materials. The observed characteristic splitting in the diffraction peaks is evidence of the tetragonal distortion in the cubic structure of the $Sr_{0.2}Ba_{0.8}TiO_3$ perovskite material [17]. Additional heat treatment for the material compositions at 900°C has revealed sharpening and enhances the intensity of all reflections. For practical purposes, all the compositions heated at 800°C were studied. It was interesting to note that with the Ba Substitution, though there was no significant shift in 2θ values was observed but a slight broadening of diffraction peaks can be seen for x = 0.40 and 0.80, confirming that Ba was perfectly introduced in the cubic structure. The crystallite size was calculated using the Debye-Scherrer formula, which estimates the size of smaller crystals from their diffraction peaks and found to be in the range of 33 to 61 nm, confirming their nano-crystalline nature.

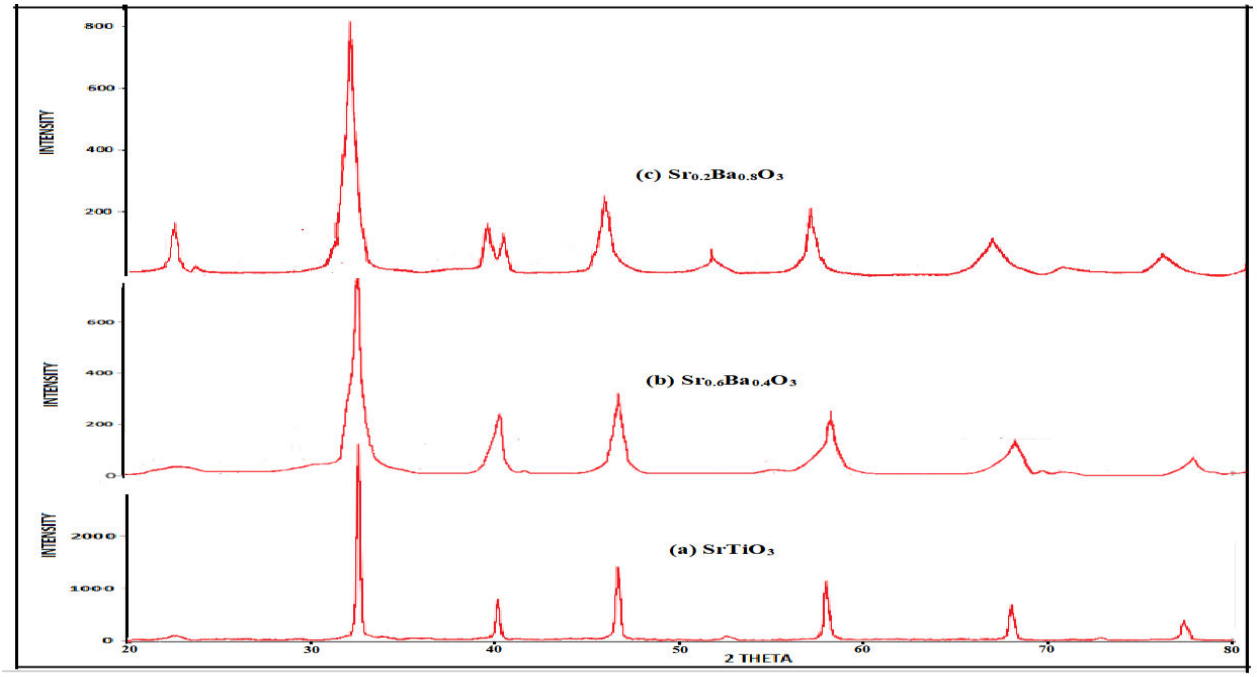

Fig. 1: XRD pattern of (a) $SrTiO_3$, (b) $Sr_{0.6}Ba_{0.4}TiO_3$, and (c) $Sr_{0.2}Ba_{0.8}TiO_3$ nanomaterials

3.2. FTIR Spectroscopy

FTIR technique detects frequencies of infrared light that are absorbed by a molecule. Fig. 2 shows FTIR Spectrum recorded in the transmitted mode for metal citrate precursors (dried at 150°C for 2 h) and their respective product $SrTiO_3$, $Sr_{0.6}Ba_{0.4}TiO_3$, and $Sr_{0.2}Ba_{0.8}TiO_3$ nanomaterials in the range of 500-4000 cm^{-1}. The vibrational peaks assigned to 540, 860, 1420, 1634, and 3410 cm^{-1} are typical peaks Sr Ba Titanate showing stretching in Ti-O (normal and bending mode). The spectrum shows the presence of broad bands centered at 3432 cm^{-1} assigned to water stretching vibrations, 1385 cm^{-1} to Ba-Ti-O bonds, to stretching modes. The absorption band at 936 cm^{-1} and 540 cm^{-1} is assigned to stretching vibrations modes of O-Ti-O and Ti-O-Ti bonds. The absorption corresponding 1634 and 3412 cm^{-1} due to -OH stretching and -OH deformation arisen due to the presence of moisture in agreement to the literature [20].

3.3. The catalytic applications of the $Sr_{1-x}Ba_xTiO_3$ nanomaterials

3.3.1. Biginelli reaction

In this investigation, we report an efficient three-component, one-pot synthesis of dihydropyrimidinone in the presence of nanomaterials under investigation, as heterogenous base catalysts. The catalytic product was confirmed by melting point (mp). Table 1 summarizes the yield obtained (%) and mp of the recrystallized dihydropyrimidinone product, confirming the formation and purity of the expected product.

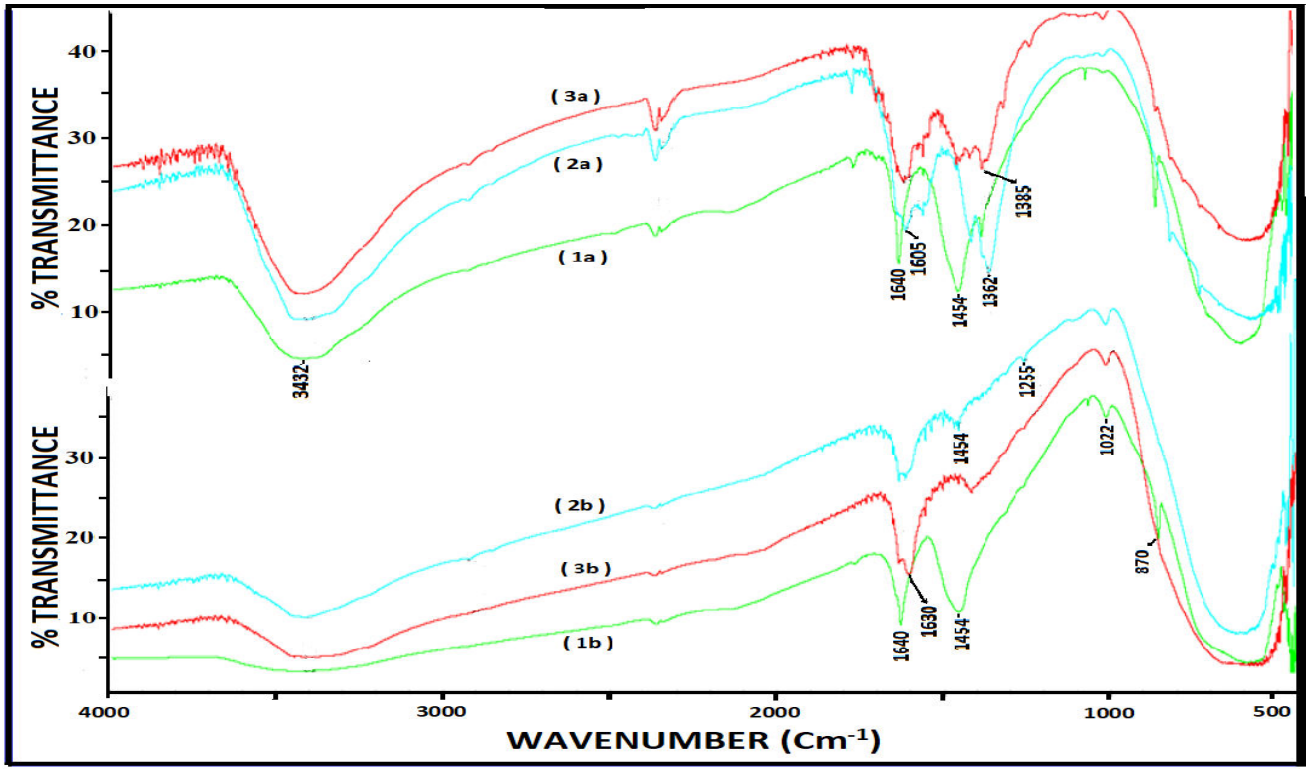

Fig. 2: FTIR absorption bands for (a) citrate precursor (b) Calcined of (1) $SrTiO_3$, (2) $Sr_{0.6}Ba_{0.4}TiO_3$, and (3) $Sr_{0.2}Ba_{0.8}TiO_3$ nanomaterials

Table 1: Yield and melting point of recrystallized dihydropyrimidinone

Nanocatalyst	Weight (in g)	% Yield	Melting point
Reference (Blank)	0.143 g	30%	201°C
$SrTiO_3$	0.209 g	41%	197°C
$Sr_{0.6}Ba_{0.4}TiO_3$	0.276 g	46%	200°C
$Sr_{0.2}Ba_{0.8}TiO_3$	0.287 g	50%	199°C

The table 1 shows the amount of recrystallized dihydropyrimidinone product and their melting points. The percentage yield is different for all the nano-catalysts. As per the above data, $Ba_{0.8}Sr_{0.2}TiO_3$ gives the best yield among the rest of the nanoparticles. The melting point of the final product was found out and when correlated to the registered data confirmed the formation of dihydropyrimidinone. The synthesized dihydropyrimidinone product was identified by comparison of melting point (mp) of 207°C, in agreement with the literature [21-23].

3.3.2. Photodegradation of Laundry wastewater

As the semi-conducting materials with bandgap energies between 1.4 and 3.8 eV are potential photocatalytic materials candidates for visible light photo-catalysts for degradation of pollutants. The prepared nanomaterials were tested on the laundry waste (LW) water containing synthetic dyes as a model reaction for photo-degradation of organic pollutants. The nanocatalysts were activated in the oven at 100°C for 1 h. 25mL each of the LW water was taken in 4 different conical flasks. λ_{max} of the LW water was found out to be 400 nm using a UV-Visible Spectrophotometer. 0.25g of the activated nanocatalysts was added in three flasks, while one flask was considered to be a reference (blank solution). The solutions were then irradiated under natural sunlight with occasional stirring and λ_{max} of the sample was then recorded every 30 min. Graph of optical density v/s time (min) was plotted.

Fig. 3 shows the photocatalytic efficiency plot of the nanocatalyst materials. All materials exhibit reasonably good LW water degradation by up to 70 % in 150 min. $SrTiO_3$ nanocatalyst show overall higher activity and highest in the first 60 mins. It was clearly seen that under identical conditions, the photo-degradation shown by $Sr_{0.6}Ba_{0.4}TiO_3$ was comparatively less than $Sr_{0.2}Ba_{0.8}$ TiO_3 nanocatalyst material. The degradation rate of LW water (blank) without catalysts was less than 2% indicating their stability under visible light. The photo-catalytic stability of these materials was confirmed by repeating the degradation experiment on the next day on the same catalyst materials, the results obtained were consistent.

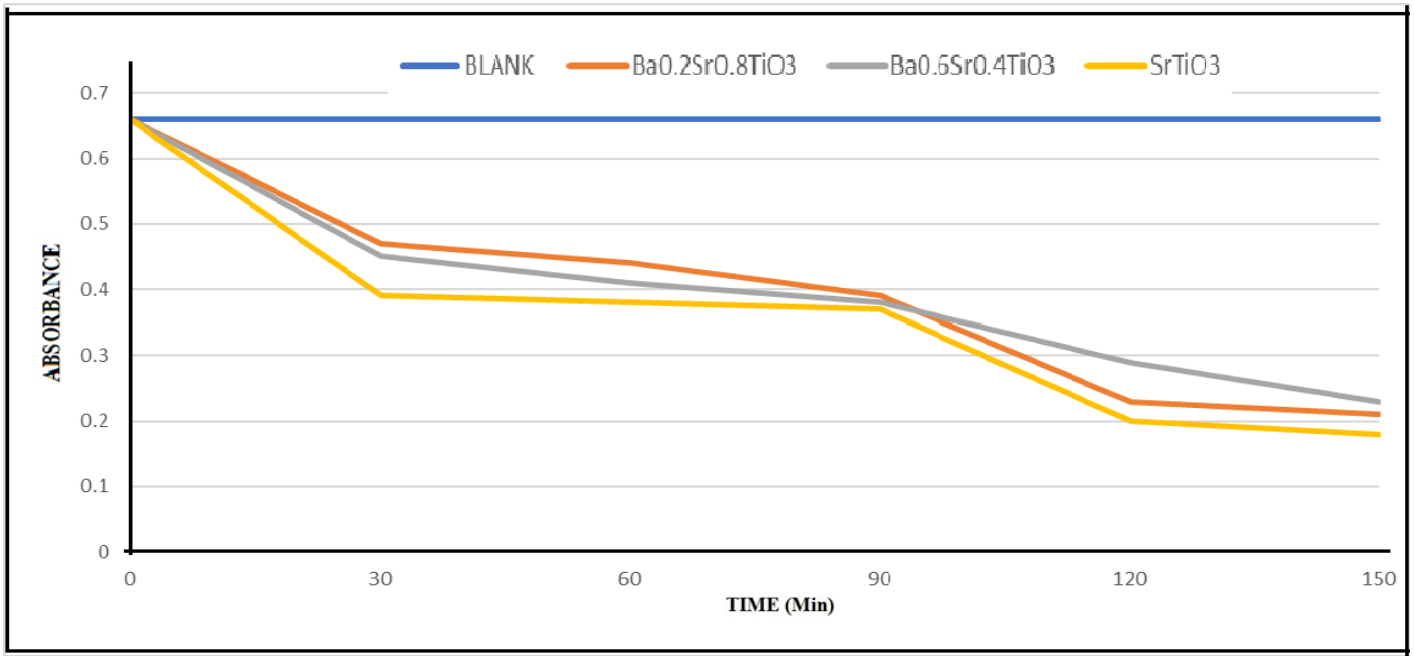

Fig. 3: Photocatalytic degradation of Laundry waste water using $SrTiO_3$, $Sr_{0.6}Ba_{0.4}TiO_3$, and $Sr_{0.2}Ba_{0.8}TiO_3$ nanomaterials

In fig. 3, the higher photocatalytic activity of $SrTiO_3$ material could be attributed to its stronger visible light absorption. As observed, the photo-degradation percentage on all nanomaterials increased rapidly, after the reaction mixture kept in direct sunlight. Within the first 60 min, it was noted appreciable degradation, as indicated by fading of dye colours and appreciable fading after 150 min. This indicates that the rupturing of conjugation bonds within the dye molecules take place due to solar light with photo-catalysts, giving colourless

products. These results illustrate that the investigated materials are potential candidates and efficient for photocatalytic applications. The particles size influences the photo-catalytic efficiency and finer particles are expected to be more efficient. The observed photo-catalysis efficiency of $SrTiO_3$ can be attributed to a finer particle size of 30 nm, as compared to the other two. The bandgap energy of $SrTiO_3$ and $BaTiO_3$ are 3.2 and 3.9 eV respectively [5, 20]. As the atomic concentration of Ti remains practically the same in all the materials, it may have an indirect role for catalytic activity. The observed photo-degradation pattern may be due to the Ba substitution and its atomic concentration in $SrTiO_3$ crystal structure. As the Ba^{+2} ions start taking the interstitial sites replacing Sr^{+2} sites, facilitating the changes in the lattice parameters, the lattice constant, and the host lattice dimensions getting larger, increasing the crystallite size, in agreement with the calculated size using Scherrer's formula. Although, $SrTiO_3$ is a regular cubic perovskite structure, with the substitution of Ba, its getting distorted to nearly tetragonal structure [18]. The narrow bandgap semiconductor nanomaterials are regarded as potential visible-light photo-catalysts, thus their chemical activity is significantly favouring their suitability for photocatalytic degradation of organic pollutants. The optical absorption activity of semiconductor materials is strongly attributed to the electronic structure [12]. These materials being semiconductor absorbs photons (visible light) energies higher than its bandgap energy, there is the excitation of electrons from the valence to the conduction band in the photo-catalyst producing electron-hole pairs. The electron-hole pairs move to the surface of the material and react with the organic dyes and finally, decomposition of the dyes take place. Therefore, the photocatalytic activity of these nano-materials is attributed to the synergistic contribution of bandgap energies, crystal structure and particle size.

4. CONCLUSION

In summary, pure crystalline pristine $SrTiO_3$ and its Ba-substituted nano-materials were synthesized with the sol-gel citrate method. A single-phase cubic perovskite structure was confirmed by X-ray powdered diffraction. It was found by XRD that Ba as a substituent, was introduced in the cubic lattice distorting it to tetragonal structure in $Sr_{0.2}Ba_{0.8}TiO_3$ due to its larger atomic size. Photo-degradation of actual laundry wastewater containing synthetic dye as pollutants using semi-conductor photo-catalyst nanomaterials with solar light can make it economically viable as the radiation source is an inexpensive, abundant, and renewable natural energy source. They are having unique semi-conducting properties that have applications in cleansing wastewater by photo-degradation of organic pollutants like various dyes, using natural sunlight. The superior photocatalytic activity of $SrTiO_3$ was attributed to the synergistic contribution of bandgap energies, crystal structure, and particle size. These nanomaterials being well-known photocatalysts were explored for the synthesis of dihydropyrimidinone and found to be efficient.

Conflict of Interests

The authors declare that they have no conflicts of interests.

5. REFERENCES

1. Tanaka H, Misono M.*Cur. Opin. Solid State Mater. Sc.*, 2001; **5(5):**381-387.
2. BhallaA, Guo R, Roy R. *Mat. Res. Innovat.,* 2000; **4:**3-26.
3. Grabowska E. *Appld. Catal. B: Environ.*, 2016; S0926-3373(15)30319-2.
4. Haeni JH, Irvin P, Chang W, Uecker R, Reiche P, Li YL, et al. *Nature*, 2004; **12(430-7001):**758-761.
5. Cen C, Thiel S, Mannhart J, Levy J. *Science*, 2009; **323(5917):**1026-1030.
6. Ortmann JE, Duncan MA, Demkov AA. *Opt. Mater. Express,* 2019; **9:**2982-2993.
7. Nath RK, Zain M, Kadhum AAH. *Adv. Nat. Appld. Sci.*, 2012; **6:**1030-1035.
8. Cai F,Tang Y, Chen F, Yan Y, Shi W. ***RSC Adv.***, 2015, 5:21290-21296.
9. Sulaeman U, Yin S, Sato T. *Appld. Catal. B: Environ.,* 2011; **105:**206-210.
10. 10.Lee DK, Cho IS, Yim DK, Noh JH, Hong KS, Kim DW. *J. Ceram. Soc. Jpn,* 2010; **118(1382):**876-880.
11. Alammar T, Hamm I, Wark M, Mudring AV. *Appld. Catal. B: Environ.*, 2015; **178:**20-28.
12. Hisatom T, Kubota J, Domen K.*Chem. Soc. Rev.*, 2014. http://doi.org/10.1039/c3cs60378d.
13. Vaz T, Salker AV. *J. Adv. Sci. Res.*, 2020; **11(4):**107-111.
14. Klaytae T, Panthong P, Thountom S.*Cer. Internl.*, 2013; **39:**S405-S408.
15. Arya PR, Jha P, Ganguli AK. *J. Mater. Chem.***,** 2003; 13:415-423.

16. Beck HP, Eiser W, Haberkorn R. *J. Eur. Ceram. Soc.,* 2001; **21:**2319-2323.
17. Saravanan VK, Raju JKC, Krishna GM, et al. *J. Mater. Sci.,* 2007; **42:**1149-1155.
18. Ioachim A, Toacsan MI, Banciu MG, Nedelcu L, et al. *Prog. Sol. St. Chem.*, 2007; **35(2-4):**513-520.
19. Cho WS.*J. Phys. Chcm. Solids,* 1998; **59(5):**659-666.
20. Singh M, Yadav BC, Ranjan A, Kaur M, Gupta SK. *Sens. Actuators B Chem.,* 2017; **241:**1170-1178.
21. Qu H, Li X, Mo F, Lin X. *Beilstein J. Org. Chem.*, 2013; **9(1):**2846-2851.
22. Peng J, Deng Y.*Tetrahedron Lett.,* 2001; **42(34):**5917-5919.
23. Oliver KC. *Acc. Chem. Res.*, 2000; **33(12):**879-888.